Article

Synthesis of Star-Branched Poly(vinyl alcohol) and Ice Recrystallization Inhibition Activity

Thomas R. Congdon,[1] Rebecca Notman[1] and Matthew I. Gibson[1,2]*

_____

[1]Prof M. I. Gibson, Dr R. Notman, Dr T. Congdon
Department of Chemistry
University of Warwick
Coventry, UK, CV4 7AL
[2]Prof. M. I. Gibson
Warwick Medical School, University of Warwick, Coventry, UK, CV4 7AL
E-mail: m.i.gibson@warwick.ac.uk

_____

Highlights

1. The design and synthesis of a simple and efficient trifunctional MADIX agent is reported.

2. Excellent VAc control was achieved and well defined 3-arm PVA stars with no crosslinking were prepared.

3. Star polymers were evaluated for their Ice Recrystallization Inhibition Activity

Antifreeze proteins are potent inhibitors of ice crystal growth (recrystallization), which is a highly desirable property for cryopreservation and other low temperature applications. It has emerged that relatively simple polymers based on poly(vinyl alcohol) can mimic this activity, but the link between architecture and activity is not known. Here, a trifunctional xanthate was designed and synthesized to prepare star-branched poly(vinyl alcohols) by RAFT/Xanthate mediated polymerization, and their ice growth inhibition activity probed for the first time. The trifunctional agent design affords the formation of well-defined star polymers, with no evidence of star-star linking, even at high conversions, and narrow molecular weight dispersity. It is observed that three-arm stars have identical activity to two-armed (*i.e.* linear) equivalents, suggesting that the total hydrodynamic size of the polymer (diameter three-arm ~ two-arm) rather than total valence of the functional groups is the key descriptor of activity.

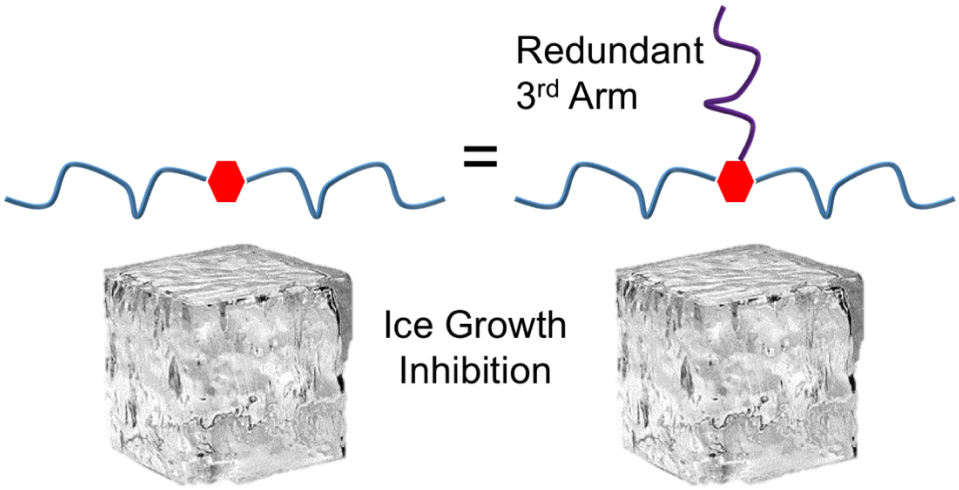

1. Introduction

Due to their similar size and diverse functionality, synthetic polymers have been widely explored to mimic the function of biomacromolecules, including proteins and polysaccharides. For example, Tew and coworkers have prepared polymers that can efficiently penetrate cell membranes in a manner similar to cell-penetrating peptides.[1] Synthetic hydrogels can mimic the extracellular matrix to prepare tailored stem cell niches,[2] or synthetic glycopolymers can mimic the cell surface glycocalyx.[3], [4] Polymers can also be used to mimic protein responses to external stimuli, for example metal concentration.[5] Antifreeze (glyco)proteins (AF(G)Ps) are specialized proteins expressed in extremophile species that enable them to survive in sub-zero climates. These proteins act to reduce the freezing point of the blood serum and show potent ice recrystallization inhibition (IRI) activity; slowing the growth of any ice crystals which form or enter circulation, that leads to a fatal build-up of ice.[6], [7] The ability to inhibit ice growth is of huge (bio)technological significance, but especially in the cryopreservation of donor cells and tissue. However, AF(G)Ps are challenging to obtain in large quantities and have had mixed results in cell storage due to unwanted ice-shaping effects.

Inada *et al.* and Budke *et al.* have demonstrated that (highly-disperse and partially acetylated) poly(vinyl alcohol) (PVA) has potent ice recrystallization inhibition (IRI) activity despite no real structural similarities to native AF(G)Ps.[8], [9] We have used controlled radical polymerization to generate well-defined PVA and elucidated that polymers comprised of as few as 10 – 20 units retained potent IRI activity.[10] This potent ice recrystallization inhibition activity was subsequently used to enhance the cryopreservation of red blood cells, by reducing ice crystal growth during the thawing stage,[11], [12], [13] and also in a solvent free system.[14] Despite these advances, and 40 years of research into AF(G)Ps, there is still much debate on the actual mechanism of antifreeze protein function, which in turn limits the ability to synthesize new biomimetic materials. Recent experiments have suggested that irreversible

binding to ice crystal is occurring with antifreeze proteins, but do not prove the link to observable macroscopic effects.[15], [16] Ben *et al.*[17] have prepared synthetic AFGP mimics which do not appear to bind the ice, but rather disrupt the interface between ice crystals; the quasi liquid layer, and posit that this gives rise to potent IRI activity. Star-branched AFPs have been found to retain their IRI activity relative to linear counterparts but show enhanced ice binding, implying a complex relationship between size and activity.[18] However, changing the macromolecular architecture or size of proteins is non-trivial (as it becomes a new protein), requiring site-specific conjugation chemistries. Conversely, due to having only a single chemically distinct repeat unit, synthetic polymers can easily be varied in terms of size and shape. Congdon *et al.* have shown that addition on a second hydrophilic block to PVA does not affect the IRI activity,[19] and Voets and coworkers have developed bottle-brush PVA's for ice growth inhibition.[20]

Due to the advances in controlled radical polymerization methods, it is now not only possible to readily access well-defined materials, but also polymers of variable architecture which enables their properties to be tuned.[21], [22] Star branched polymers typically have smaller solution dimensions and lower intrinsic viscosity compared to the corresponding linear polymer, and also display more end-groups, which may affect their ice interactions.[23], [24] For these reasons, probing the effect of branching and viscosity will give a greater understanding as to the factors affecting ice recrystallization inhibition. The effect of viscosity is especially intriguing, as with linear polymers viscosity is dependent on polymer size, whereas with star polymers it is possible to access comparable viscosities, but at higher molecular weights. Stenzel and coworkers have developed multifunctional xanthates to enable (star) polymerization of lesser activated monomers such as vinyl acetate, which are typically harder to polymerize then methacrylate monomers. These multifunctional xanthates displayed a tendancy to form star-star couples, leading to an increase in dispersity and poorly defined

polymer products. This was due to the configuration of the xanthates on the multifunctional agent. [25], [26], [27]

Considering the above, this manuscript describes the design, synthesis and use of a novel multifunctional MADIX agent designed with a configuration that allows the polymers to grow from the core. This approach affords well-defined three-armed polymers with no star-star coupling. When using these stars as an IRI agent, activity is maintained, opening the door to increasingly complex IRI active materials and tools to understanding the ice/water interface.

2. Experimental Section

Materials

4,4′-azobis(4-cyanovaleric) acid (80%), benzyl bromide (98%), deuterated chloroform (99.8 atom% D), deuterium oxide (99.9 atom% D), potassium ethyl xanthate (96%), 1,3,5-tris(bromomethyl)benzene (99%), vinyl acetate (99%), and all solvents were purchased from Sigma Aldrich. Hydrazine hydrate solution (80%) was purchased from Fisher Scientific. Phosphate-buffered saline (PBS) solutions were prepared using preformulated tablets (Sigma-Aldrich) in 200 mL of MilliQ water (>18.2 Ω mean resistivity) to give [NaCl] = 0.138 M, [KCl] = 0.0027 M and pH 7.4. Methyl(ethoxycarbonothioyl)sulfanyl benzene was prepared according to literature methods.[28]

Analytical and physical methods

^{1}H and ^{13}C NMR spectra were recorded on Bruker DPX-300 and DPX-400 spectrometers using deuterated solvents purchased from Sigma-Aldrich. Chemical shifts are reported relative to residual non-deuterated solvent. Size exclusion chromatography (SEC) was used to examine and differentiate between the molecular weights and dispersities of the synthesized polymers. SEC analysis was performed on a Varian 390-LC MDS system equipped with a PL-AS RT/MT

autosampler, a PL-gel 3 μm (50 × 7.5 mm) guard column, two PL-gel 5 μm (300 × 7.5 mm) mixed-D columns held at 30 °C and the instrument equipped with a differential refractive index and a Shimadzu SPD-M20A diode array detector. The mobile phase was THF with 5 % triethylamine (TEA) eluent at a flow of 1.0 mL/min, and samples were calibrated against Varian Polymer Laboratories Easi-Vials linear poly(styrene) and poly(methyl methacrylate) standards (162-2.4 x 10^5 g/mol) using Cirrus v3.3. Ice wafers were annealed on a Linkam Biological Cryostage BCS196 with T95-Linkpad system controller equipped with a LNP95-Liquid nitrogen cooling pump, using liquid nitrogen as the coolant (Linkam Scientific Instruments UK, Surrey, UK). An Olympus CX41 microscope equipped with a UIS-2 20x/0.45/∞/0-2/FN22 lens (Olympus Ltd, Southend on sea, UK) and a Canon EOS 500D SLR digital camera was used to obtain all images. Image processing was conducted using Image J, which is freely available from http://imagej.nih.gov/ij/.

'Splat' (ice recrystallization inhibition) Assay

Ice recrystallization inhibition was measured using a modified splay assay.[29] A 10 μL sample of polymer dissolved in PBS buffer (pH 7.4) was dropped 1.40 m onto a chilled glass coverslip sat on a piece of polished aluminum placed on dry ice. Upon hitting the chilled glass coverslip, a wafer with a diameter of approximately 10 mm and a thickness of 10 μm was formed instantaneously. The glass coverslip was transferred onto the Linkam cryostage and held at - 8 °C under N_2 for 30 minutes. Photographs were obtained using an Olympus CX 41 microscope with a UIS-2 20x/0.45/∞/0-2/FN22 lens and crossed polarizers (Olympus Ltd, Southend on sea, UK), equipped with a Canon DSLR 500D digital camera. Images were taken of the initial wafer (to ensure that a polycrystalline sample had been obtained) and after 30 minutes. Image processing was conducted using Image J,[30] which is freely available. Four of the largest ice crystals were measured and the single largest length in any axis recorded. This was repeated for three wafers and the average (mean) value was calculated to find the largest grain dimension

along any axis. The average of this value from three individual wafers was calculated to give the mean largest grain size (MLGS).

Synthesis of Synthesis of 1,3,5 tris-(methylethoxycarbonothioyl sulfanyl) benzene

Potassium ethyl xanthate (5.00 g, 0.031 mol, 3.0 eq) was added to ethanol (120 mL) in a round bottom flask and stirred at 60 °C until the solid had fully dissolved. 1,3,5 tris (methylbromo)benzene (3.71 g, 0.01 moles, 1.0 eq) was added to the stirred solution in a single portion and the reaction stirred at 60 °C for 6 h, forming a pale yellow solution and a white precipitate. The mixture was filtered to remove the salt and then ethanol was removed *in vacuo* leaving a yellow oil and a white solid. The mixture was dissolved in DCM (150 mL) and the product precipitated upon the addition of small amounts of water (10 mL). The product was filtered leaving a white solid, which was then thoroughly dried under vacuum using a schlenk line apparatus, furnishing the product as a white solid. Yield 2.69 g 56 %, ^{1}H NMR ($CDCl_3$): δ = 7.23 (3H, s, benzyl ring), 4.65 (6H, q, J = 6.8 Hz, OCH_2), 4.31 (6H, s, SH_2), 1.42 (9H, t, J = 8 Hz, CH_3). ^{13}C NMR ($CDCl_3$): δ = 136.0 (*ipso* C), 128.0 (benzyl *C*H), 70.2 (S*C*H_2), 39.9 (O*C*H_2), 13.8 (*C*H_3). ESI MS; 480.9 Da $[M+H]^+$, 502.9 Da $[M + Na]^+$, 518.9 Da $[M + K]^+$ Expected [M]: 480.0.

Polymerization of Vinyl Acetate using 1,3,5 tris-(methylethoxycarbonothioyl sulfanyl) benzene

As a representative example, 1,3,5 tris-(methylethoxycarbonothioyl sulfanyl) benzene (0.015 g, 0.03 mmol), vinyl acetate (2.81 g, 0.33 mol), and ACVA (4,4′-azobis(4-cyanovaleric acid); (0.082 g, 33 mol%) were added to a stoppered vial equipped with a stir bar. The solution was thoroughly degassed under a flow of N_2 for 20 min, and the reaction mixture was then allowed to polymerise at 68 °C for typically 15 h. The yellow solutions were then cooled to room

temperature. Poly(vinyl acetate) was then recovered as a yellow sticky solid after precipitation into hexane. The hexane was then decanted and the poly(vinyl acetate) was re-dissolved in THF, which was then concentrated *in vacuo* and thoroughly dried under vacuum at 40 °C for 24 h, forming a white crystalline solid. Representative characterization data for ***Star*-PVAc$_{87}$**: ^{1}H NMR (400 MHz, $CDCl_3$) δ = 7.16 (benzyl *H*, s, 3H), 4.61 (-C*H*O-CH_2, br, 90H), 4.42 (-CH_2CH$_3$, q, 6H), 4.24 (-CH_2S-, s, 6H), 1.74 (-CO-CH_3, br, 270H), 1.53 (-CH_2-, br, 180H); M_n^{SEC}(THF) = 7420 Da, M_w/M_n = 1.18.

Hydrolysis of Star-poly(vinyl acetate) to Star-poly(vinyl alcohol)

As a representative example, 3-arm *star*-poly(vinyl acetate) (1.0 g, 7420 Da, M_n/M_w = 1.18) was dissolved in a methanol (5 mL) and hydrazine hydrate solution (10 mL, 80% in water) in a round-bottom flask. The reaction mixture was stirred at 30 °C for 4 h, and was then dialysed using distilled water and 3-arm *star*-poly(vinyl alcohol) was recovered as a spongy white solid by freeze-drying the dialysis solution. Hydrazinolysis was determined by ^{1}H NMR Spectroscopy. Representative characterization data for ***Star*-PVA$_{87}$**: ^{1}H NMR (400 MHz, $CDCl_3$) δ = 7.16 (benzyl *H*, s, 3H), 4.00 (−C*H*OH–, br, 90), 1.68–1.60 (−CH_2–, br, 180H).

Polymerisation of Vinyl Acetate using Methyl(ethoxycarbonothioyl)sulfanyl benzene

As a representative example Methyl(ethoxycarbonothioyl)sulfanyl benzene (0.21 g, 0.99 mmol), vinyl acetate (4.67 g, 2.64 mmol) and ACVA (4,4'-azobis(4-cyanovaleric acid)) (0.013 g) were added to a stoppered vial. The solution was thoroughly degassed under a flow of N_2 for 20 mins and the reaction mixture was then allowed to polymerize at 68 °C for typically 15 h. The yellow solutions were then cooled to room temperature. Poly(vinyl acetate) was then recovered as a yellow sticky solid after precipitation into hexane. The hexane was then decanted and the poly(vinyl acetate) was re-dissolved in THF, which was then concentrated *in vacuo* and thoroughly dried under vacuum at 40 °C for 24 h, forming a white crystalline solid.

Representative characterization data for **$PVAc_{81}$**: ^{1}H NMR (400 MHz, $CDCl_3$): δ=4.61 (-C*H*O-CH_2 br 1H), δ=1.74 (-CO-C*H*$_3$ br 3H), δ=1.53 (-C*H*$_2$- br 2H), M_n^{SEC}(THF) = 7010 Da, M_w/M_n = 1.19.

Hydrolysis of Poly(vinyl acetate) to Poly(vinyl alcohol)

As a representative example, poly(vinyl acetate) (1.5 g, 3300 Da, M_n/M_w = 1.22) was dissolved in a methanol (20 mL) and hydrazine hydrate solution (15 mL, 80 % in water) in a round bottom flask. The reaction mixture was stirred at 30 °C for 2 h. The reaction mixture was then dialysed using distilled water and poly(vinyl alcohol) was recovered as a spongy white solid by freeze drying the dialysis solution. Deacetylation was determined by ^{1}H NMR. Representative characterization data for **PVA_{81}**: ^{1}H NMR (400 MHz, $CDCl_3$): δ=4.00 (-C*H*OH- br 1H), δ=1.68-1.60 (-C*H*$_2$- br 2H).

3. Results and Discussion

In order to access well-defined star branched PVA *via* RAFT/MADIX polymerization a multifunctional xanthate (chain transfer agent) was required. A new tri-functional xanthate was designed such that the 'R' group is on the core, ensuring the polymer chains remain attached after deprotection of the acetate groups, **Scheme 1**. The other advantage of this design is that the 'core first' propagation of the polymer chain affords well-defined 3-arm stars with little variation in the molecular weight of each arm (as evidenced through viscometric analysis), and the lack of any star-star coupling, even at high conversions. The xanthate was synthesized by the reaction of potassium ethyl xanthate and 1,3,5-tris-bromomethylbenzene to give 1,3,5 tris-(methylethoxycarbonothioyl sulfanyl) benzene in > 50 % yield, without the need for column chromatography. It is interesting to point out that, under these conditions, only the trifunctional product is formed, hence the need for only a minimal work-up to afford pure RAFT agent. The xanthate was subsequently used for the polymerization of vinyl acetate in bulk with ACVA (4,4'-azobis(4 cyanovaleric acid)) as the radical source. Following isolation, these star-PVAcs were characterized by NMR spectroscopy and SEC, revealing a controlled polymerization by the observed control of molecular weight and low dispersity values. SEC traces are shown in **Figure 1A**. The acetate protecting groups were quantitatively removed by hydrazine hydrate, as confirmed by ^{1}H NMR spectroscopic analysis (ESI). Full details of the resultant polymers are shown in **Table 1**. Each PVA is labelled according to the average length of each arm, not the total size of the polymer, to aid in analyzing the IRI activity of each polymer, *vide infra*.

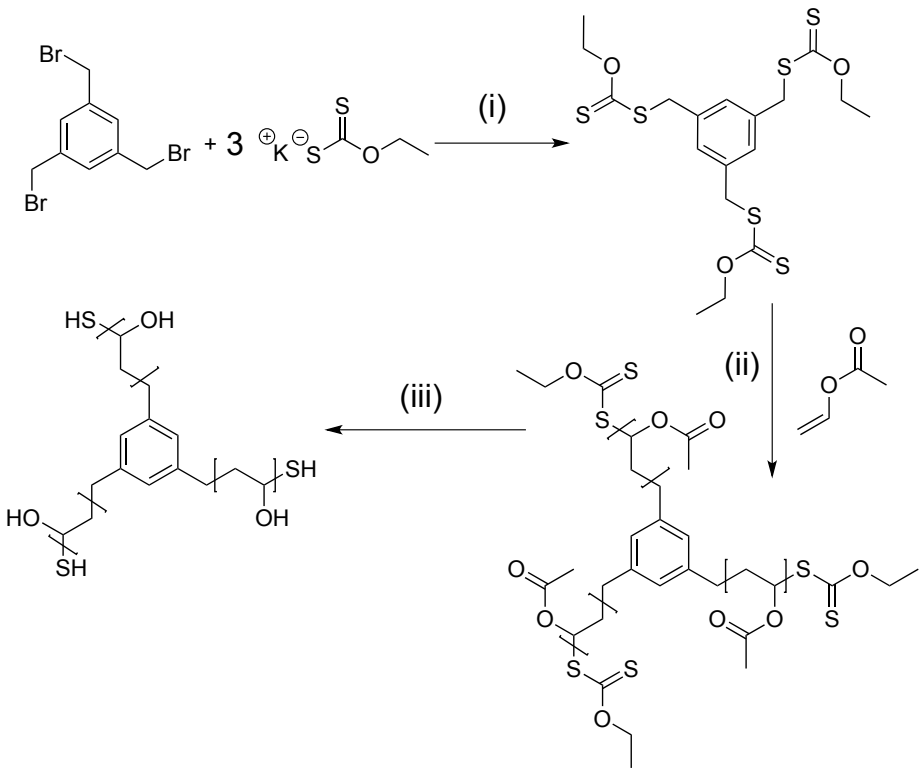

Scheme 1. Synthesis of star-PVAs. (i) EtOH, 60 °C, 3 hr; (ii) ACVA, 68 °C ; (iii) H_2N_4, MeOH/H_2O, 60 °C 3 h.

To confirm that the polymers were indeed star branched, viscometric SEC analysis was conducted (star branched polymers have lower intrinsic viscosity than their linear equivalents, due to their more compact shape in solution). The resultant Mark-Houwink plot of ***Star*-PVA$_{27}$** against a linear PVA with similar molecular weight and dispersity **(Figure 2B)** confirms the branched morphology of the star polymers.

As can be seen in **Figure 1B**, the star polymer showed lower intrinsic viscosity than the corresponding linear polymer at all molecular weight fractions. This implies that the polymer is branched, and that the number of 'dead arms' is minimal. The overall difference between the two polymers is limited due to their relatively low molecular weight. This low M_n range (< 10 g.mol^{-1}) was essential to enable discrimination in the IRI activity assays, as our previous work has indicated this is the region of greatest M_n dependence on activity.[10]

Table 1. Star Polymers

***Star*-PVAc**	**[M]:[CTA] [a)] (-)**	**Conv [b)] (%)**	**$M_{n,}^{NMR\ b)}$ ($g.mol^{-1}$)**	**$M_{n,}^{SEC\ c)}$ ($g.mol^{-1}$)**	**$Đ$ [c)] (-)**	**DP_n [d)] (-)**	**DP_{Arm} [e)] (-)**	***Star*-PVA [f)]**
***Star*-PVAc$_6$**	30	36	1290	1560	1.12	18	6	***Star*-PVA$_6$**
***Star*-PVAc$_{16}$**	48	94	4050	4300	1.34	48	16	***Star*-PVA$_{16}$**
***Star*-PVAc$_{21}$**	220	30	5680	5490	1.35	63	21	***Star*-PVA$_{21}$**
***Star*-PVAc$_{27}$**	58	95	6460	7060	1.28	81	27	***Star*-PVA$_{27}$**
***Star*-PVAc$_{30}$**	120	78	6200	7420	1.18	87	30	***Star*-PVA$_{30}$**
***Star*-PVAc$_{45}$**	180	82	13300	11800	1.41	138	45	***Star*-PVA$_{45}$**
***Star*-PVAc$_{78}$**	270	94	21900	20200	1.38	234	78	***Star*-PVA$_{78}$**
***Star*-PVAc$_{99}$**	330	94	26700	25700	1.42	299	99	***Star*-PVA$_{99}$**

a) Monomer to RAFT agent ratio; **b)** Determined by ^{1}H NMR spectroscopy; **c)** Determined by SEC in THF using PMMA standards; **d)** Number-average degree of polymerization; **e)** Number-average degree of polymerization per arm; **f)** Corresponding PVA prepared by hydrolysis of the respective PVAc star polymer.

With this library of star-branched polymers to hand, IRI activity was evaluated using a 'splat' assay. Briefly, 10 μL drops of the polymer in PBS saline, (pH = 7.4) were rapidly frozen (- 80 °C) to generate a polynucleated wafer of ice. This was then annealed at - 6 °C for 30 minutes before being photographed and the mean largest grain size (MLGS) measured and reported relative to a PBS control, to give a % MLGS relative to PBS. Small values indicate more IRI activity. The results of this assay are shown in **Figure 2**. Note, not all the star polymers were tested, but rather a range of sizes until the activity had plateaued (based on our previous studies of linear PVA) suggesting that any further increases in molecular weight would not give significant differences in activity.

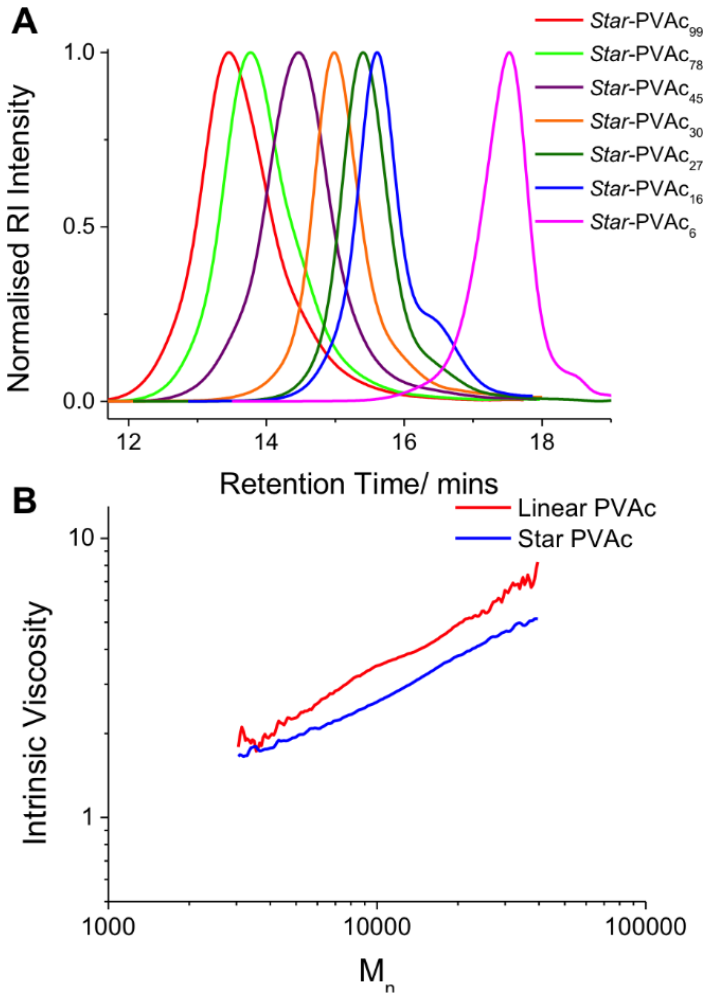

Figure 1. A) SEC in THF traces for 3-arm *star*-poly(vinyl acetate) polymers prepared for this study. B) Mark-Houwink plot of 3-arm star PVAc and linear PVAc with similar M_n and Đ. Linear PVAc (DP_n 81, M_n = 7010, Đ = 1.19). Star PVAc (DP_n 81, DP_A = 27, M_n = 7060 Đ = 1.29).

The data shown in **Figure 2A** reveals that the star branched PVAs retained their IRI activity despite the change in macromolecular architecture from linear to branched. Of the polymers tested, *Star*-PVA_{16} showed the lowest activity compared to the other, longer polymers. This is a similar observation to linear polymers, which show a clear M_n-related activity trend, with higher molecular weight PVAs displaying greater IRI activity. Whilst the overall activity of *Star*-PVA_{16} is low, it should be noted that this is in the dilute concentration range and at concentrations above 1 $mg.mL^{-1}$ all the polymers fully inhibited ice growth, highlighting

PVA's remarkable IRI activity, compared to any other polymeric IRI agents. Example micrographs showing the concentration-dependence on IRI activity are shown in **Figures 2B – 2D**.

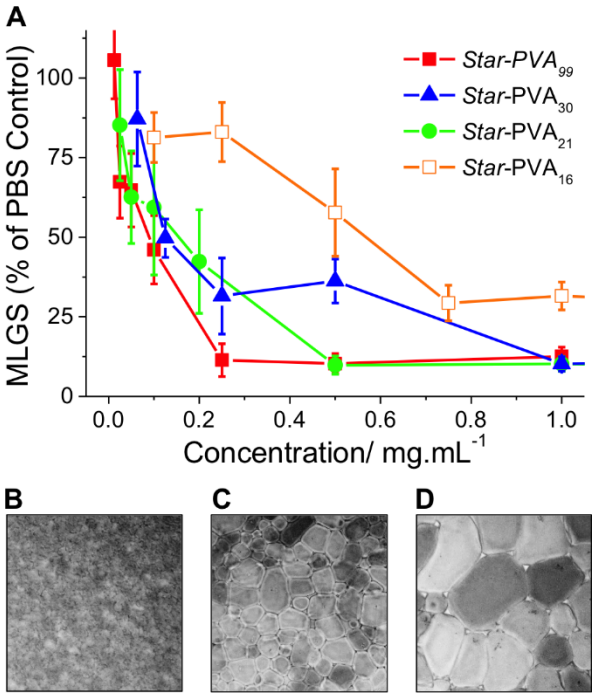

Figure 2. A) Ice recrystallization inhibition activity of star-PVA polymers. Representative cryo-micrographs of *Star*-PVA21 at 0.5 (B), 0.2 (C) and 0.01 mg.mL^{-1}(D). All images 300 μm wide. Error bars are ± standard deviation from n ≥ 3.

The activity of the star-branched polymers may give some insight into the mechanisms of IRI; it is unclear how native AF(G)Ps function, and the huge structural differences between them and PVA raise more questions. There is evidence that high molecular weight PVA can shape growing ice crystals, implying a direct surface interaction with specific crystal planes. However, there is no direct link between extant of 'binding' and IRI activity. In fact, evidence from Ben *et al*. suggests that IRI activity and ice binding are completely independent of each

other, but that AF(G)Ps perform both.[17], [31] One current hypothesis is that compounds that display IRI activity inhibit the transfer of water from the quasi-liquid layer to bulk, limiting ice growth.[32] If the PVA was binding to the ice then it might be expected that a three-armed star polymer would be a more avid binder than a 'two-armed star' (i.e. linear polymer) due to the increased number of functional groups. **Figure 3** shows a comparison of PVA of similar total molecular weight but different architecture (star and linear). Across the series there are no significant differences in activity, which supports the concept that PVA's IRI activity might not be dependent on ice crystal binding (at least, not at these concentrations), or that ice binding is not the sole contribution to activity. Our observations would also appear to rule out that the IRI activity of PVA is due to an increased viscosity of the eutectic phase between ice crystals (or the branched polymers would be less active). Similar trends were seen across the whole data set (longer PVAs), which is included in the ESI.

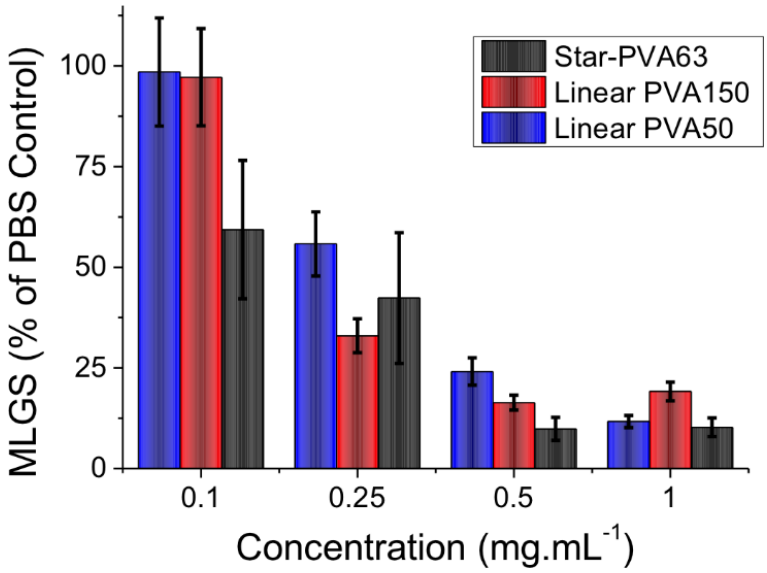

Figure 3. Comparison of the IRI activity of linear verses star branched PVA's. Error bars are ± standard deviation from $n \geq 3$. Note, Star-PVA63 corresponds to Star-PVA_{21}, The DP_n value has been used in this case to aid direct comparison of polymers of similar chain length.

The fact that activity is preserved upon changing the architecture is particularly useful in the design of more complex AFP mimetic materials; for example, to introduce biodegradability or sensory components into the structure. It also highlights the intrinsic complexity of the ice growth process and the subtle effects polymer structure has on activity.

Conclusions

A novel trifunctional xanthate was designed to prepare well-defined 3-arm stars of PVA. The agent was synthesized from cheap starting materials and was isolated pure as a trifunctional xanthate, without the need for column chromatography. The xanthate was taken on and employed for the controlled polymerization of vinyl acetate, which after deprotection enabled access to library of well-defined three-armed star poly(vinyl alcohol)s. These branched polymers were found to maintain the potent ice recrystallization inhibition activity found in linear PVA. Three-armed stars showed no increase in activity, compared to a two-armed equivalent. This result was surprising as increasing the molecular weight of linear polymers is strongly correlated with increased ice recrystallization inhibition activity. Due to the compact dimensions of a three-arm star compared to a similar molecular weight linear polymer, it can be seen that hydrodynamic size rather than total valency (of polymer repeat units) is the crucial factor for activity. We propose that this supports the theory that these polymers do not require binding to the ice crystals to inhibit growth, but rather function to disrupt the transfer of water between ice crystal interfaces. These findings highlight the simplicity and utility of preparing multifunctional xanthates, and will aid the development of new, more active and functional polymeric ice recrystallization inhibitors, which will find application in cellular cryopreservation and other ice-rich environments.

Acknowledgements

Equipment used was supported by the Innovative Uses for Advanced Materials in the Modern World (AM2), with support from Advantage West Midlands (AWM) and part funded by the European Regional Development Fund (ERDF). The Leverhulme Trust are thanked for a

research project grant (RPG-144). MIG acknowledges the ERC for a starter grant (CRYOMAT 638661).

Keywords: ice, antifreeze, star polymers, RAFT polymerization, poly(vinyl alcohol)

References

[1] A. Som, A. Reuter, G. N. Tew, *Angew. Chem. Int. Ed.* **2012**, *51*, 980-983.
[2] H. Geckil, F. Xu, X. Zhang, S. Moon, U. Demirci, *Nanomedicine (London, England)* **2010**, *5*, 469-484.
[3] M. W. Jones, L. Otten, S. J. Richards, R. Lowery, D. J. Phillips, D. M. Haddleton, M. I. Gibson, *Chem. Sci.* **2014**, *5*, 1611-1616.
[4] D. Rabuka, M. B. Forstner, J. T. Groves, C. R. Bertozzi, *J. Am. Chem. Soc.* **2008**, *130*, 5947-5953.
[5] D. J. Phillips, G.-L. Davies, M. I. Gibson, *J. Mater. Chem. B* **2015**, *3*, 270-275.
[6] Y. Yeh, R. E. Feeney, *Chem. Rev.* **1996**, *96*, 601-618.
[7] N. M. Tsvetkova, B. L. Phillips, V. V. Krishnan, R. E. Feeney, W. H. Fink, J. H. Crowe, S. H. Risbud, F. Tablin, Y. Yeh, *Biophys. J.* **2002**, *82*, 464-473.
[8] S. S. Lu, T. Inada, A. Yabe, X. Zhang, S. Grandum, *Int. J. Refrig.* **2002**, *25*, 562-568.
[9] C. Budke, T. Koop, *Chemphyschem* **2006**, *7*, 2601-2606.
[10] T. Congdon, R. Notman, M. I. Gibson, *Biomacromolecules* **2013**, *14*, 1578-1586.
[11] R. C. Deller, M. Vatish, D. A. Mitchell, M. I. Gibson, *Nat. Commun.* **2014**, *5*, DOI:10.1038/ncomms4244.
[12] D. E. Mitchell, M. Lilliman, S. G. Spain, M. I. Gibson, *Biomaterials Sci.* **2014**, *2*, 1787-1795.
[13] R. C. Deller, J. E. Pessin, M. Vatish, D. A. Mitchell, M. I. Gibson, *Biomaterials Sci.* **2016**, *8*, 824-833.
[14] D. E. Mitchell, J. R. Lovett, S. P. Armes, M. I. Gibson, *Angew. Chem. Int. Edit.* **2016**, *55*, 2801-2804.
[15] T. Sun, F.-H. Lin, R. L. Campbell, J. S. Allingham, P. L. Davies, *Science* **2014**, *343*, 795-798.
[16] C. P. Garnham, R. L. Campbell, P. L. Davies, *P. Natal. Acad. Sci. USA* **2011**, *108*, 7363-7367.
[17] A. K. Balcerzak, C. J. Capicciotti, J. G. Briard, R. N. Ben, *RSC Advances* **2014**, *4*, 42682-42696.
[18] C. A. Stevens, R. Drori, S. Zalis, I. Braslavsky, P. L. Davies, *Bioconjugate Chem.* **2015**, *26*, 1908-1915.
[19] T. R. Congdon, R. Notman, M. I. Gibson, *Biomacromolecules* **2016**. DOI:10.1021/acs.biomac.6b00915
[20] L. L. C. Olijve, M. M. R. M. Hendrix, I. K. Voets, *Macromol. Chem. Physic.* **2016**, *217*, 951-958.

[21] R. T. A. Mayadunne, J. Jeffery, G. Moad, E. Rizzardo, *Macromolecules* **2003**, *36*, 1505-1513.
[22] Y. K. Chong, T. P. T. Le, G. Moad, E. Rizzardo, S. H. Thang, *Macromolecules* **1999**, *32*, 2071-2074.
[23] L. J. Fetters, A. D. Kiss, D. S. Pearson, G. F. Quack, F. J. Vitus, *Macromolecules* **1993**, *26*, 647-654.
[24] G. Lapienis, *Prog. Polym. Sci.* **2009**, *34*, 852-892.
[25] M. H. Stenzel, T. P. Davis, C. Barner-Kowollik, *Chem. Commun.* **2004**, 1546-1547.
[26] J. Bernard, A. Favier, L. Zhang, A. Nilasaroya, T. P. Davis, C. Barner-Kowollik, M. H. Stenzel, *Macromolecules* **2005**, *38*, 5475-5484.
[27] C. Barner-Kowollik, T. P. Davis, M. H. Stenzel, *Aust. J. Chem.* **2006**, *59*, 719-727.
[28] J. Skey, R. K. O'Reilly, *Chem. Commun.* **2008**, 4183-4185.
[29] C. A. Knight, D. Wen, R. A. Laursen, *Cryobiology* **1995**, *32*, 23-34.
[30] C. A. Schneider, W. S. Rasband, K. W. Eliceiri, *Nat. Methods* **2012**, *9*, 671 - 675.
[31] C. J. Capicciotti, M. Leclere, F. A. Perras, D. L. Bryce, H. Paulin, J. Harden, Y. Liu, R. N. Ben, *Chem. Sci.* **2012**, *3*, 1408-1416.
[32] R. Y. Tam, C. N. Rowley, I. Petrov, T. Zhang, N. A. Afagh, T. K. Woo, R. N. Ben, *J. Am. Chem. Soc.* **2009**, *131*, 15745-15753.